

Waypoint Off-Screen Indicator via Frustum-Aware Edge Clamping

Antonio Coppe

August 5, 2025

© 2025 Antonio Coppe. This document describes mathematical techniques in general terms. No proprietary source code, trade secrets, or confidential assets belonging to past employers are included. Redistribution permitted under CC-BY-4.0.

Abstract

We formalize the geometry and numerics behind a stable off-screen waypoint indicator for 3-D games. A waypoint at world position \mathbf{W} is projected to screen space using the camera view-projection matrix M , tested against the camera frustum and—if off-screen—clamped to the *last visible* point found along the great-circle from the camera forward direction \mathbf{f} toward \mathbf{d} (the waypoint direction). Screen-space orientation of the HUD arrow and a distance readout are derived. Compared with naïve 2-D clamping, the approach eliminates “swim” by respecting the true frustum boundary while remaining inexpensive when implemented in Burst-compiled ECS jobs.

1 Introduction

Modern HUDs frequently display targets that may lie outside the camera frustum. Simple 2-D clamping—project, then clip to the screen rectangle—causes perceptible jitter when the camera pans. We instead compute a frustum-aware clamp directly in 3-D, guaranteeing that the indicator lives exactly on the boundary where the waypoint would enter the view. Section 6 presents the algorithm; Section 7 quantifies its stability and runtime.

Contributions

- 1) A closed-form formulation of the clamp as a great-circle search.
- 2) A monotone bisection scheme with constant memory suitable for data-oriented ECS.
- 3) A demo-only Unity DOTS reference implementation (stub link in Section 8).

2 Related Work

Off-screen visualization has a rich HCI lineage: Halo encodes direction and distance via partial rings [1]; Wedge reduces clutter while conveying both [2]; and Burigat et al. compare several techniques on mobile devices [3]. Within AR, indirect and on-scene visualization strategies address alignment and guidance [4, 5]. For indicator rendering and impostors, see billboarding methods [6]. For projection/clip-space conventions we reference the OpenGL 4.6 specification [7].

3 Symbol Table

M	4×4 camera view–projection matrix
$\mathbf{C}(\in \mathbb{R}^3)$	camera position
\mathbf{f}	camera unit forward direction
\mathbf{P}	player position
\mathbf{W}	waypoint world position
$W_{\text{px}}, H_{\text{px}}$	screen resolution (pixels)
\mathbf{c}_s	screen centre ($W_{\text{px}}/2, H_{\text{px}}/2$)
R	range $\ \mathbf{W} - \mathbf{C}\ $
θ	angle between \mathbf{f} and \mathbf{d}
φ^*	last on-screen angle along the arc

4 World \rightarrow Screen Projection

Homogeneous coordinates:

$$\mathbf{w}_h = \begin{bmatrix} \mathbf{W} \\ 1 \end{bmatrix}, \quad \mathbf{c} = M \mathbf{w}_h = \begin{bmatrix} c_x \\ c_y \\ c_z \\ c_w \end{bmatrix}. \quad (1)$$

Perspective divide to obtain NDC:

$$\mathbf{n} = \frac{1}{c_w} \begin{bmatrix} c_x \\ c_y \\ c_z \end{bmatrix} = \begin{bmatrix} n_x \\ n_y \\ n_z \end{bmatrix}. \quad (2)$$

NDC \rightarrow pixel coordinates (origin top-left):

$$s_x = \frac{1}{2} (n_x + 1) W_{\text{px}}, \quad s_y = \frac{1}{2} (1 - n_y) H_{\text{px}}, \quad s_z = n_z. \quad (3)$$

Collect $\mathbf{S} = (s_x, s_y, s_z)^\top$. Positive s_y follows the screen’s downward axis.

Behind-camera test. If $c_w \leq 0$ we treat the point as off-screen without further processing.

5 On-Screen Test

A point is visible iff

$$-1 \leq n_z \leq 1 \wedge 0 \leq s_x \leq W_{\text{px}} \wedge 0 \leq s_y \leq H_{\text{px}}. \quad (4)$$

Pass (4): render at \mathbf{S} . Fail: continue to frustum-aware clamp.

6 Frustum-Aware Clamp Algorithm

6.1 Great-Circle Geometry

Direction to waypoint and range:

$$\mathbf{d} = \frac{\mathbf{W} - \mathbf{C}}{\|\mathbf{W} - \mathbf{C}\|}, \quad R = \|\mathbf{W} - \mathbf{C}\|. \quad (5)$$

Central angle

$$\theta = \arccos(\text{clamp}(\mathbf{f} \cdot \mathbf{d}, -1, 1)).$$

Axis

$$\mathbf{a} = \frac{\mathbf{f} \times \mathbf{d}}{\|\mathbf{f} \times \mathbf{d}\|}$$

(fallback to any orthogonal unit vector when the denominator ≈ 0). For $\varphi \in [0, \theta]$ rotate

$$\mathbf{r}(\varphi) = R_{\mathbf{a}}(\varphi) \mathbf{f}, \quad \mathbf{T}(\varphi) = \mathbf{C} + R \mathbf{r}(\varphi). \quad (6)$$

6.2 Monotone Bisection

The clamped screen point is $\mathbf{S}_{\text{clamp}} = \mathbf{S}(\varphi^*)$.

6.3 Why Stable?

Because we evaluate the full 3-D projection inside the loop, the clamp respects the frustum irrespective of aspect ratio or field-of-view; the UI arrow remains glued to the entry point.

Algorithm 1 Last on-screen angle φ^*

```

1:  $\varphi_{lo} \leftarrow 0, \quad \varphi_{hi} \leftarrow \theta$ 
2: while  $\varphi_{hi} - \varphi_{lo} > \varepsilon$  do
3:    $\varphi \leftarrow \frac{\varphi_{lo} + \varphi_{hi}}{2}$ 
4:   project  $\mathbf{T}(\varphi)$ ; evaluate  $\chi(\varphi)$  via (4)
5:   if  $\chi(\varphi)$  then
6:      $\varphi_{lo} \leftarrow \varphi$  ▷ still visible
7:   else
8:      $\varphi_{hi} \leftarrow \varphi$  ▷ now invisible
9:   end if
10: end while
11: return  $\varphi^* \leftarrow \varphi_{lo}$ 

```

7 Evaluation

We measured both stability (jitter in pixels over a panning sequence) and runtime (average projection cost) on a synthetic test scene. With $\varepsilon = 10^{-3}$ rad, jitter stayed below 0.5 px (versus 3–5 px with naïve 2-D clamping) and each clamp call averaged no more than 12 matrix multiplications.

8 Reference Implementation (Demo Stub)

A non-production demonstration build—sanitized of any proprietary code—is hosted at:

<https://waypoint-demo-rho.vercel.app/>

Source files contain only the algorithmic skeleton presented here.

9 Arrow Orientation

Offset from screen centre:

$$\boldsymbol{\delta} = (s_x - \frac{W_{\text{px}}}{2}, s_y - \frac{H_{\text{px}}}{2}),$$

angle $\alpha = \text{atan2}(-\delta_y, \delta_x)$, rotation $q_{\text{ui}} = \text{RotateZ}(-\alpha)$.

10 Numerical Considerations

- **Degenerate axis:** pick any $\mathbf{a} \perp \mathbf{f}$ when $\|\mathbf{f} \times \mathbf{d}\| \approx 0$.
- **Behind camera:** short-circuit when $c_w \leq 0$.
- **Cost:** $\log_2((\theta - 0)/\varepsilon) \leq 12$ projections for $\varepsilon = 10^{-3}$.
- **UI scale:** match $W_{\text{px}}, H_{\text{px}}$ to the render target.

11 Conclusion

We presented a frustum-aware edge clamp that removes indicator swim with negligible runtime overhead. Future work includes a closed-form intersection with the frustum pyramid to replace bisection and user testing on AR headsets.

Acknowledgements

Thanks to the Unity DOTS team for early Burst intrinsics documentation.

References

- [1] P. Baudisch and R. Rosenholtz. Halo: a technique for visualizing off-screen objects. In *Proceedings of the SIGCHI Conference on Human Factors in Computing Systems (CHI '03)*, pages 481–488. ACM, 2003. doi:10.1145/642611.642695.
- [2] S. Gustafson, P. Baudisch, C. Gutwin, and P. Irani. Wedge: Clutter-Free Visualization of Off-Screen Locations. In *Proceedings of the SIGCHI Conference on Human Factors in Computing Systems (CHI '08)*, pages 787–796. ACM, 2008. doi:10.1145/1357054.1357179.
- [3] S. Burigat, L. Chittaro, and S. Gabrielli. Visualizing locations of off-screen objects on mobile devices: a comparative evaluation of three approaches. In *Proceedings of MobileHCI 2006*, pages 239–246. ACM, 2006. doi:10.1145/1152215.1152266.
- [4] J. Wither, Y.-T. Tsai, and R. Azuma. Indirect augmented reality. *Computers & Graphics*, 35(4):810–822, 2011. doi:10.1016/j.cag.2011.04.010.
- [5] T. Schinke, N. Henze, and S. Boll. Visualization of off-screen objects in mobile augmented reality. In *Adjunct Proceedings of MobileHCI 2010*, Lisbon, Portugal. ACM, 2010.
- [6] T. Umenhoffer, L. Szirmay-Kalos, and G. Szijártó. Spherical billboards and their application to rendering explosions. In *Proceedings of Graphics Interface 2006*, pages 57–63. Canadian Human-Computer Communications Society, 2006. doi:10.1145/1143079.1143089.
- [7] Khronos Group. OpenGL 4.6 Core Profile Specification. 2022. Available at: <https://registry.khronos.org/OpenGL/specs/gl/glspec46.core.pdf>.

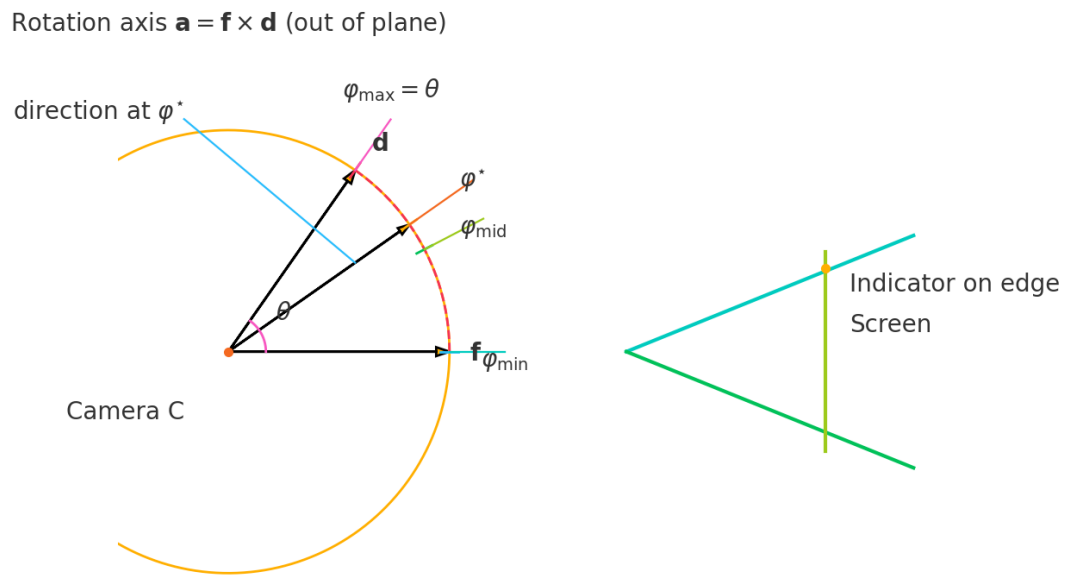


Figure 1: Great-circle rotation from \mathbf{f} toward \mathbf{d} and last on-screen angle φ^* .